Proceedings of the ASME 2017 36th International Conference on Ocean, Offshore and Arctic Engineering
OMAE2017
June 25-30, 2017, Trondheim, Norway

OMAE2017-61766

PREDICTION OF COMBINED IL AND CF VIV RESPONSE OF DEEPWATER RISERS

Jie Wu
SINTEF Ocean [1]
Trondheim, Norway

Malakonda Reddy Lekkala
Department of Mechanical and Structural Engineering and Materials Science
University of Stavanger
Stavanger, Norway

Muk Chen Ong
Department of Mechanical and Structural Engineering and Materials Science
University of Stavanger
Stavanger, Norway

Elizabeth Passano
SINTEF Ocean [1]
Trondheim, Norway

Per Erlend Voie
DNV GL
Trondheim, Norway

ABSTRACT

Deepwater risers are susceptible to Vortex Induced Vibrations (VIV) when subjected to currents. When responding at high modes, fatigue damage the in in-line (IL) direction may become equally important as the cross-flow (CF) components. If a riser experiences directional currents, fatigue damage must be evaluated at several locations on the cross-section's circumference. Accurate calculation of both IL and CF responses are therefore needed.

Empirical VIV prediction programs, such as VIVANA, SHEAR7 and VIVA, are the most common tools used by the offshore industry to design against VIV loads. Progress has been seen in the prediction of CF responses. Efforts have also been made to include an IL load model in VIVANA. A set of excitation coefficient parameters were obtained from rigid cylinder test and adjusted using measured responses of one of the flexible cylinder VIV tests. This set of excitation coefficient parameters is still considered preliminary and further validation is required. Without an accurate IL response prediction, a conservative approach in VIV analysis has to be followed, i.e. all current profiles have to assumed to be uni-directional or acting in the same direction.

The purpose of the present paper is to provide a reliable combined IL and CF load model for the empirical VIV prediction programs. VIV prediction using the existing combined IL and CF load model in VIVANA is validated against selected flexible cylinder test data. A case study of a deepwater top tension riser (TTR) has been carried out. The results indicate VIV fatigue damage [1] using 2D directional current profiles is less conservative compared to the traditional way of using uni-directional current profiles.

NOMENCLATURE

VIV	Vortex induced vibration
CF	Cross-flow
IL	In-line
D	Diameter of the bare riser (m)
U	Towing speed (m/s)
f_{osc}	Oscillation frequency (Hz)
$\bar{f}$	Non-dimensional frequency, $\bar{f} = \frac{f_{osc}D}{U}$
$\bar{f}_n$	Non-dimensional frequency corresponding to the n^{th} eigen-frequency
$M_{x,y}$	Bending moment (Nm)
I_{xx}, I_{yy}	Second moment of area (m^4)
σ	Stress (MPa)
θ	Angle around the cross-section's circumference (deg)
p	Probability of occurrence
$\bar{a}, m$	SN curve parameters
Dam	Fatigue damage (1/year)
Life	Fatigue life (year)

[1] Formerly MARINTEK. SINTEF Ocean from January 1st 2017 through an internal merger in the SINTEF Group

INTRODUCTION

Vortex shedding will generate oscillating forces, which cause structure to vibrate in the directions perpendicular to (CF) and parallel to (IL) the local flow direction. VIV can lead to a rapid accumulation of fatigue damage to slender marine structures.

Current speed and spatial patterns in the field can vary over the water column. For risers with constant orientation over the service life, such as a production riser, current conditions should be applied with the angle of attack according to the directional distribution of current in VIV prediction. While, current heading for a drilling riser is assumed to be evenly distributed. However, it is common practice to perform pure CF VIV analysis with uni-directional current profiles. This means that the fatigue damage hot spot will be concentrated in the CF direction, which can be over-conservative. This is partially due to the lack of a reliable model in present VIV prediction programs for prediction of combined IL and CF responses. It is still difficult to develop a model that covers VIV for fully 3D current profiles. However, a simplified combined IL and CF response calculation model has been made available in VIVANA (Passano et al, 2012).

Model tests with flexible cylinders have been one of the important ways to investigate VIV response. The cylinder model in most of these tests, such as the Hanøytangen experimental program (Huse et al, 1998) and the Norwegian Deepwater Program (NDP; Trim et al, 2005), is exposed to two-dimensional (2D) flow profile.

In the present study, the existing combined IL and CF load model in VIVANA has been validated against the NDP test data. The accuracy of the fatigue damage prediction around the cross-section's circumference is evaluated. A case study of a deep water top tension riser is carried out to examine the differences in VIV fatigue damage calculation using uni-directional and 2D directional current profiles.

SEMI-EMPRICAL VIV PREDICTION PROGRAM VIVANA

The VIVANA program is a semi-empirical frequency domain program based on the finite element method. The program was developed by SINTEF Ocean (formerly MARINTEK) and the Norwegian University of Science and Technology (NTNU) to predict VIV responses. The fluid-structure interaction in VIVANA is described using added mass, excitation and damping coefficients. In addition to pure CF response analysis, the program can also predict pure IL response, which occur at low current levels, before the onset of CF VIV response.

Recently, VIV response calculation due to simultaneous CF and IL excitation has been included in VIVANA. The IL response frequency is fixed at twice the CF response frequency and the IL added mass is adjusted so that this frequency becomes an eigenfrequency. A set of curves based on forces measured during combined cross-flow and in-line motions are used. At present, the IL excitation curves are not dependent on the CF response amplitude. All analyses in the present study were carried out using VIVANA 4.8.

Calculation Procedure

The program is based on the assumption that the response will occur at one or more discrete response frequencies and that these frequencies are eigenfrequencies. The system dynamic equilibrium equation is solved in frequency domain. The corresponding mode is used as the initial estimate of the response and response iterations carried out at each frequency until the response and the VIV loads are consistent with each other. The analysis consists of the following main steps:

- ***Calculation of eigenfrequencies that are possible response frequencies.***
  As the added mass is dependent on the non-dimensional frequency, $\bar{f} = \frac{f_{osc}D}{U}$, iterations are carried out for each response frequency to ensure that the added mass and the resulting eigenfrequency are consistent.
- ***Calculation of response at each response frequency.***
  The response frequency is kept constant and iterations are carried out until the response and the excitation are consistent.
- ***Calculation of resulting response, stresses and fatigue damage from all response frequencies.***
  Competing response frequencies may either appear concurrently or consecutively (time sharing).

Hydrodynamic Force Coefficients

The analysis model is based on empirical coefficients for lift force, added mass and damping. All coefficients will depend on the non-dimensional frequency. Both diameter and flow speed may vary along the riser, which means that all coefficients also may vary.

The excitation coefficient will depend on the oscillation amplitude as well as on the frequency. A positive excitation coefficient represents positive energy transfer from the fluid to the structure. The excitation coefficient becomes negative with increasing response amplitude, which means energy dissipation. This reflects the self-limiting nature of the VIV response process.

The Venugopal's damping model (1996) is used in VIVANA. This model applies different formulations for damping in high and low flow velocity regions. Figure 1 illustrates the energy balance of a riser in a sheared flow.

The added mass coefficient is assumed to be independent of the amplitude and is therefore given as a simple function of the frequency only. A constant added mass 1.0 in CF direction is used in the present study.

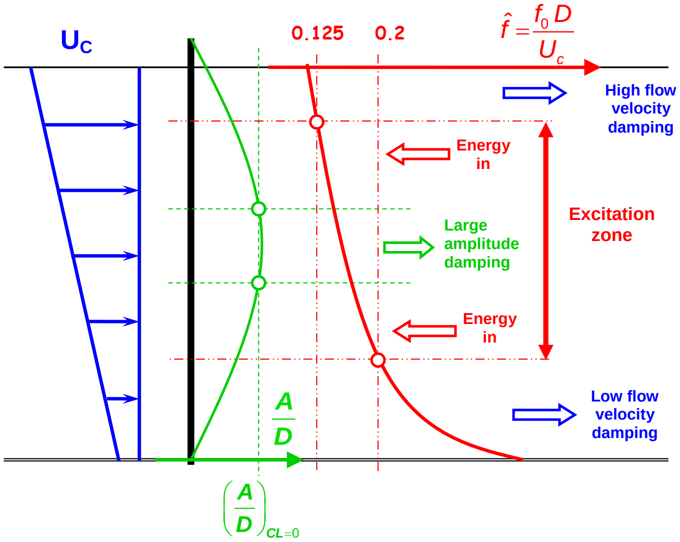

Figure 1 Energy balance for a riser vibrating in a sheared flow profile, Baarholm et al (2006)

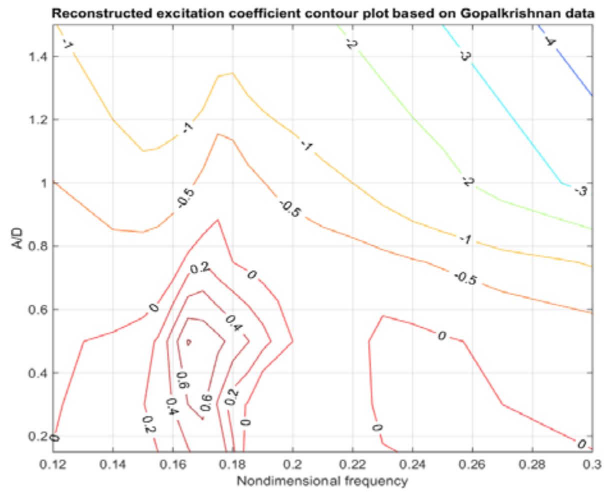

Figure 2 CF excitation coefficient contour plots reconstructed from rigid cylinder pure CF test data taken from Gopalkrishnan (1992)

1) CF Excitation Coefficient

The CF excitation coefficient is originally based on rigid cylinder forced motion test data. The excitation coefficients generated from Gopalkrishnan's (1992) test are presented in Figure 2. In such tests, the cylinder was forced to move in the CF direction only. However, the study of flexible cylinder VIV test data shows that hydrodynamic force coefficients are strongly influenced by the motion orbits of the cross-section (Wu et al, 2016). Combined IL and CF motion rigid cylinder tests (Dahl, 2008, Soni, 2008 and Yin, 2013) have also been carried out to provide data for different oscillation orbits. However, these hydrodynamic data are still considered inadequate to describe the true hydrodynamic forces of a flexible riser responding simultaneously in both IL and CF directions.

VIV test data with flexible cylinders have been used to improve the hydrodynamic force coefficient database (Wu et al, 2010, Wu, 2011) An effort to consolidate the CF excitation coefficients based on existing rigid and flexible cylinder VIV test data has been made (Voie et al, 2017). The obtained CF excitation coefficient contour plot is presented in Figure 3. It can be seen that the new excitation coefficients are significantly different than those from rigid cylinder pure CF test data, refer to Figure 2. The new force coefficients are used in the CF response predictions in the present study.

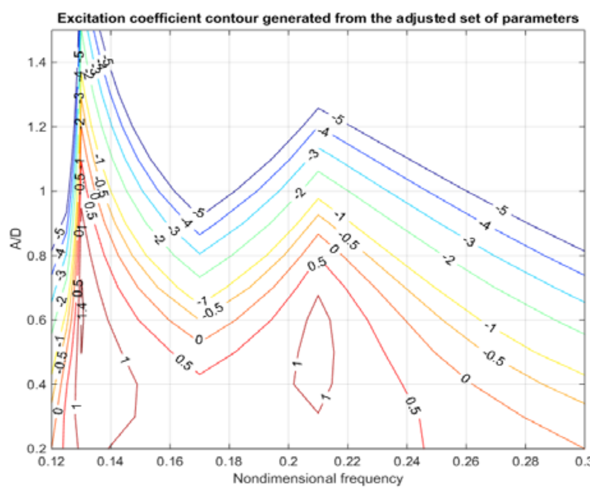

Figure 3 CF excitation coefficient contour plot generated from the adjusted set of parameters based on flexible cylinder VIV test data. The data are taken from Voie et al, (2017)

2) IL Excitation Coefficient

The IL excitation coefficients are based on Soni's (2008) experiments, but adjusted based on the flexible cylinder test data (Passano et al, 2012). The generated IL excitation coefficient contour plot is presented in Figure 4.

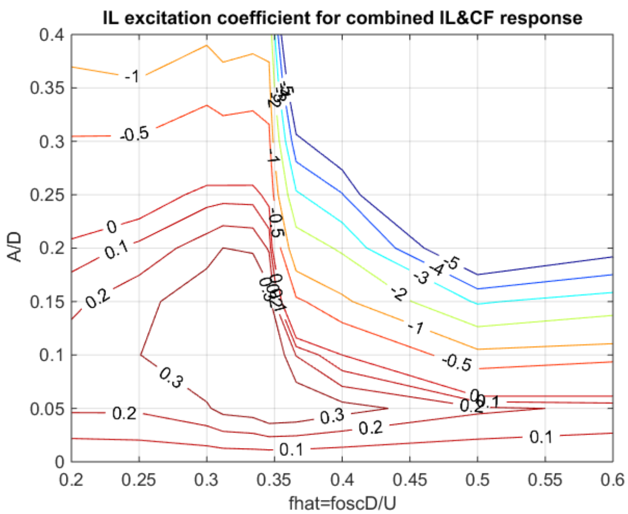

Figure 4 IL excitation coefficient (for combined IL and CF responses) contour plots. The data are taken from Passano et al, (2014a).

Stress and Fatigue Calculation around the Cross-section

The stress around the cross section of the riser is calculated using the equation below.

$$\sigma(\theta) = \frac{1}{2I_{xx}} D\sin(\theta) M_x + \frac{1}{2I_{yy}} D\cos(\theta) M_y$$

Where θ is the angle. M_y and M_x are the bending moment caused by CF and IL VIV responses, respectively. The CF and IL stress σ_θ can be found at $\theta = 0$ and 90 deg respectively. D is the external diameter. I_{xx} and I_{yy} are the second moment of area around x and y axis.

REVIEW OF NDP 38M RISER VIV MODEL TEST

SINTEF Ocean performed the tests in the Ocean Basin using a 38 m long riser model. Figure 6 shows the NDP VIV test setup. The bare riser model was a 27 mm diameter reinforced fiberglass pipe with a wall thickness of 3 mm. The test campaign includes tests with bare and straked riser models, subjected to uniform and linearly sheared flow profiles. The boundary conditions at both ends of the pipe can be approximated as pinned-pinned condition.

A total of 24 CF and 40 IL strain gauges and 8 CF and 8 IL accelerometers were utilized, creating one of the most detailed instrumentation arrays to date for measuring riser VIV response.

The test data has been extensively studied. Trim et al, (2005) reported the response mode, frequency, displacement amplitude from the model test. Fatigue damage in the IL and CF directions was also evaluated.

In the present study, the model test results of 22 bare cylinder cases with sheared flow profiles have been selected to compare with numerical predictions. The dominating frequency/mode, displacement amplitude were extracted from previous study by Baarholm (2006). Further analysis has also been carried out to evaluate the fatigue damage around the circumference of the cross-section of the test riser. The SN curve parameters used in the fatigue analysis are presented in Table 1. The higher harmonics have been filtered out before the fatigue damage is calculated for the experiments. The rain-flow counting method (WAFO 2000) was applied.

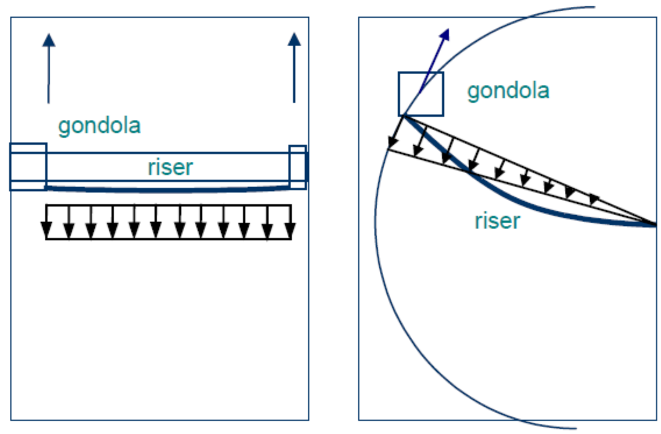

Figure 5 The NDP VIV test setup

Table 1 SN curve parameters

Parameter	Value
S-N curve	DNV F2 single slope log ā= 11.63; m=3.0
SCFs	1.0 everywhere
Notes: 1. log (N)=log ā-m • log(s), where N is the predicted number of cycles to failure under stress range S (Mpa) m is the inverse slope of the SN curve log used in the notation is log to the base 10	

VALIDATION OF COMBINED IL AND CF VIV RESPONSE PREDICTION

IL and CF responses, e.g. mode, frequency, displacement and fatigue damage were calculated using VIVANA and compared with the NDP test data. The comparison is presented for 22 sheared flow cases. The highest towing speed is 2.4 m/s. The concurrent response frequency analysis option was applied in the present study, which means that different response frequencies can be excited simultaneously at different, non-overlapping riser sections. An earlier study also demonstrates the use of consecutive response frequency (time-sharing) analysis option (Passano et al, 2014b).

The comparison of the dominating CF and IL response frequency are presented in Figure 6 and Figure 7, respectively. The measured and predicted response frequency are plotted against the maximum towing speed. It can be seen that the CF and IL frequencies are in general accurately predicted.

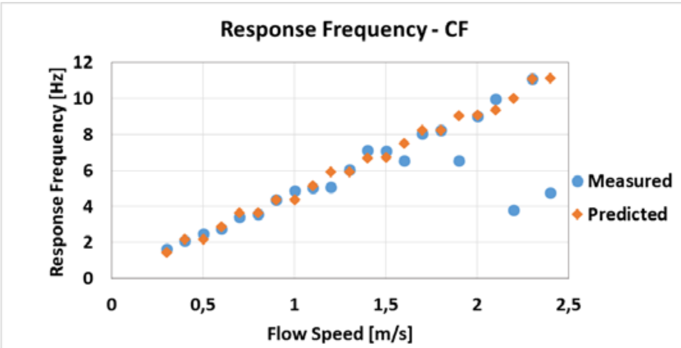

Figure 6 CF dominating frequency comparison

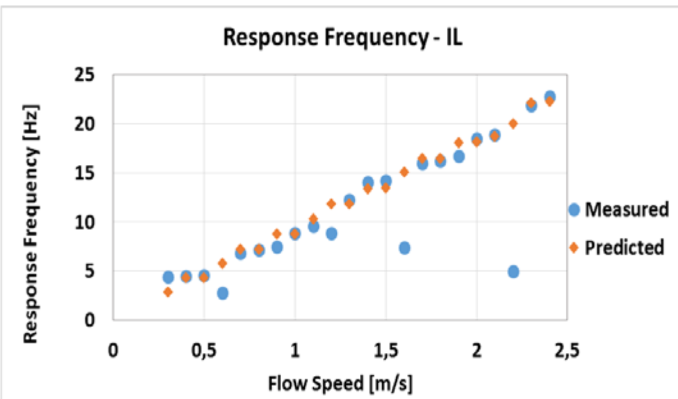

Figure 7 IL dominating frequency comparison

The comparison of the CF and IL dominating mode is presented in Figure 8 and Figure 9. Good agreement is seen in the dominating CF mode. The dominating IL mode seems to be over-predicted especially at higher towing speeds. However, the uncertainty in the data analysis also increases with higher response modes.

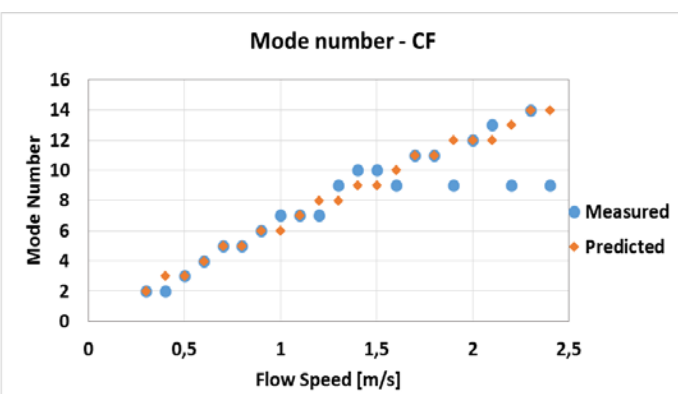

Figure 8 CF dominating mode comparison

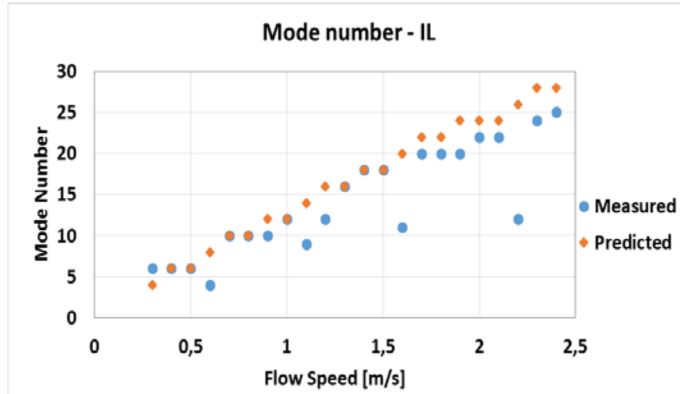

Figure 9 IL dominating mode comparison

The comparisons of the maximum CF and IL displacement amplitude ratios over the riser model are presented in Figure 10 and Figure 11, respectively. Large under-prediction of the IL responses is observed. The largest difference can be a factor of 2.5. This can lead to difference in fatigue damage by a factor of $2.5^m \approx 16$ (m=3).

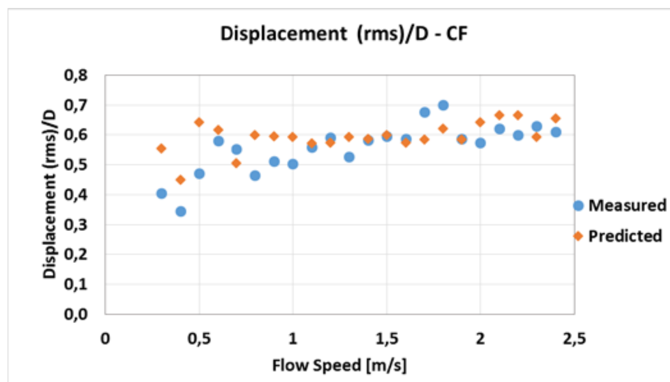

Figure 10 CF maximum displacement over diameter ratio comparison

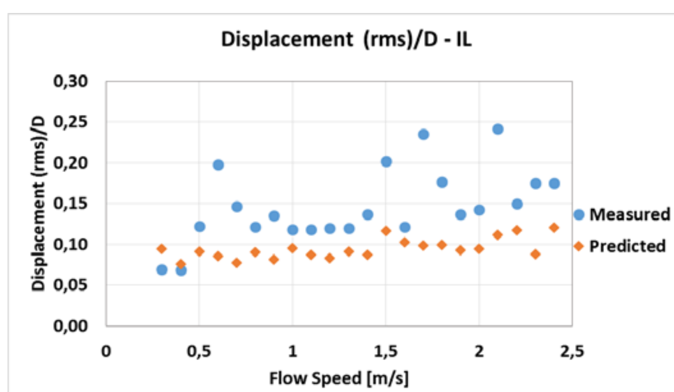

Figure 11 IL maximum displacement over diameter ratio comparison

The fatigue damage was calculated at 16 evenly spaced points around the cross-section's circumference, including CF and IL directions. Note that higher harmonics in the measurement data were filtered out before the fatigue calculation.

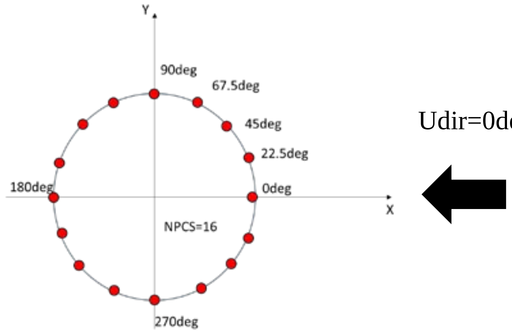

Figure 12 Points around the circumference

The predicted maximum fatigue damage for each case is presented in Figure 13. It can be seen that the CF fatigue damage is higher than the damage in the IL direction.

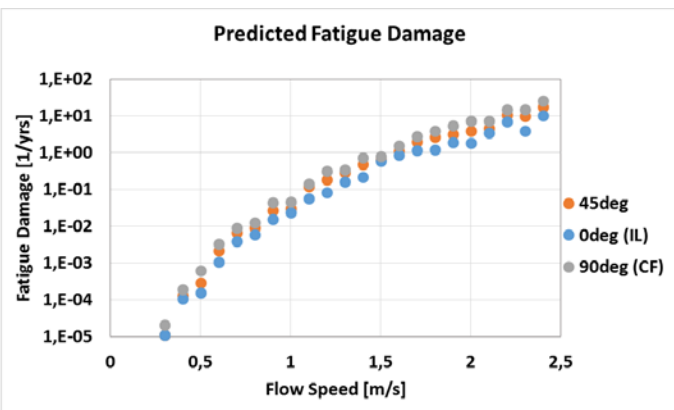

Figure 13 Predicted maximum fatigue damage

The predicted maximum CF fatigue damage agrees well with measurements and the differences are within a factor of 3 for 90% of the cases, as shown in Figure 14. The IL fatigue damage presented in Figure 15 has good agreement with measurement as well. The difference in fatigue damage comparison is within a factor of 3 for 70% of the cases. The largest difference is a factor of 10 for the case with towing speed of 1.7 m/s. The fatigue damage comparison at 45 deg around the cross-section is presented in Figure 16. In general, the difference is with in a factor of 3 for 90% of the cases. Such accuracy is considered satisfactory.

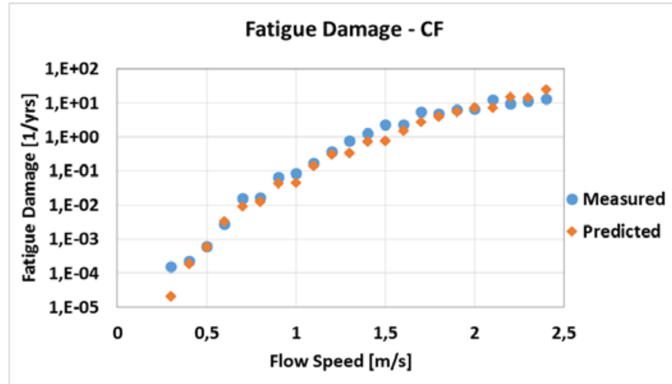

Figure 14 CF (0deg) maximum fatigue damage comparison

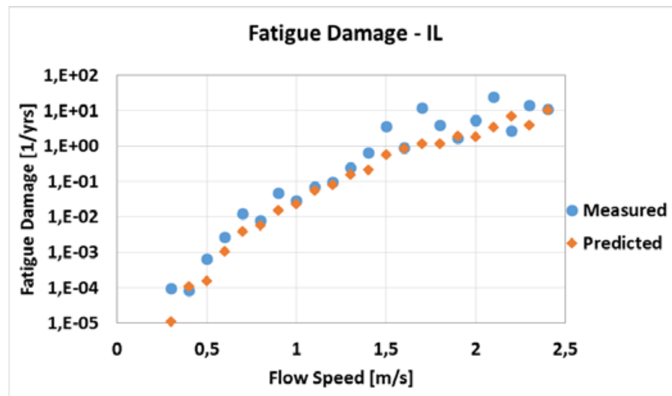

Figure 15 IL (90deg) maximum fatigue damage comparison

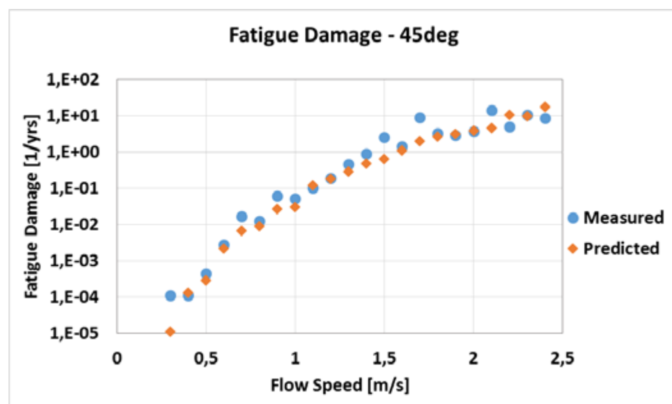

Figure 16 Maximum fatigue damage at 45 deg around the cross-section comparison

The comparison shows that the existing combined IL and CF load model in VIVANA can predict VIV responses of a flexible cylinder model with good accuracy. The fatigue damage prediction around the cross-section of the cylinder agrees well with the measurement data.

CASE STUDY OF A TOP TESNION RISER SUBJECTED TO 2D CURRENT

Case study of a deep water top tension riser is carried out to examine the differences in predicted VIV fatigue damage using uni-directional and 2D directional current profiles. The water depth is 1500 m. The riser data can be found in Annex A.

Fatigue damage will be concentrating on the direction perpendicular to the flow direction (CF) when the pure CF analysis was performed with uni-directional current profiles. When 2D directional current profiles are used in the analysis, the fatigue damage is summed at 16 evenly spaced spots on the riser circumference. The current angle of attack is constant along the pipe. The 21 current profiles are presented in Figure 17, each with an associated probability of occurrence. The current speed from 1200 m to 1500 m is linearly extrapolated.

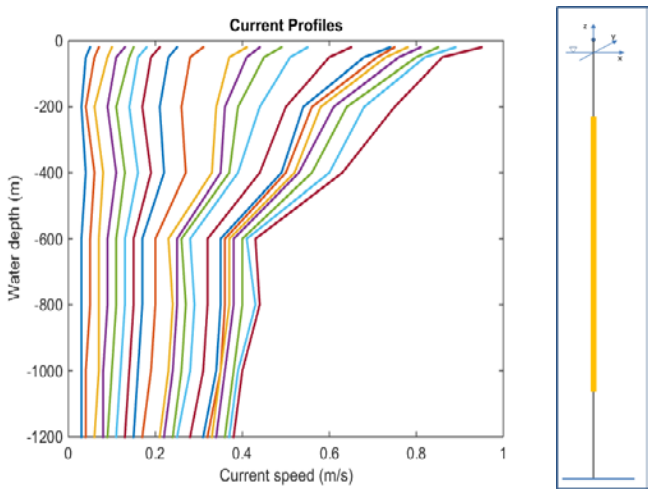

Figure 17 Current profiles

The predicted CF and IL displacement standard deviation along the riser for 21 current profiles are presented in Figure 18. The maximum displacement can be reduced due to the response mode shifts with increasing flow speeds. The dominating CF frequency corresponds to 11th mode for the highest current speed case. It is in the same response mode order compared to the NDP test results described in the previous section. It is known that the model test was carried out at sub-critical Reynolds number. The corresponding hydrodynamic force coefficients may not represent those for a riser in the field in critical Reynolds number regime (Voie et al, 2017). However, the Reynolds number effect is not considered in the present study.

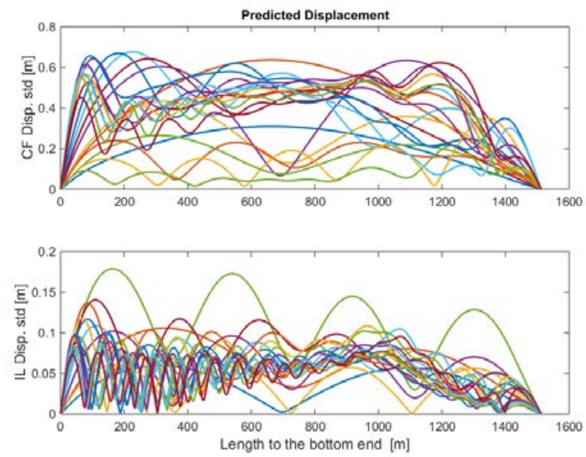

Figure 18 Predicted displacement standard deviation of a TTR for 21 current profiles

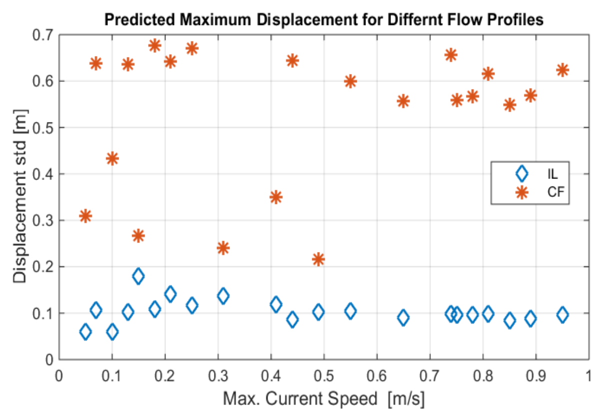

Figure 19 Predicted maximum displacement standard deviation of a TTR

The predicted maximum fatigue damage is plotted against the maximum flow speed in Figure 20. Fatigue damage was calculated at 16 evenly distributed locations around the circumstance of the cross-section. The maximum fatigue damage for 4 of the locations are shown in the figure. CF fatigue damage is higher than the damage at IL direction for 75% of cases.

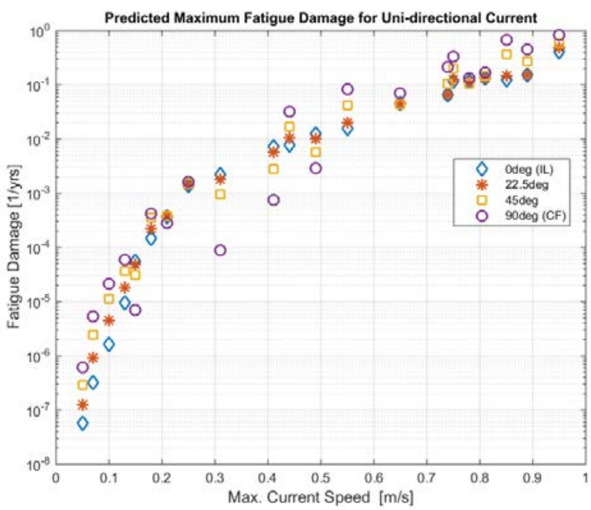

Figure 20 Predicted maximum fatigue damage at four points around the cross-section of a TTR subjected to uni-directional current (Heading: 0 deg)

The fatigue damage is accumulated at 16 points around the circumstance of the cross-section. When a pure CF response calculation with uni-directional current profiles is applied, the fatigue damage will be concentrate on the CF direction. The fatigue life can be estimated by the equation below:

$$\boldsymbol{life(z) = 1/\sum_{ic=1}^{21}(Dam(z,ic) * p(ic))}$$

where $Dam(z, ic)$ is the fatigue damage at riser location z for a given current profile ic and p is the probability of occurrence for different current profiles.

It is now assumed that the heading of the current has the same probability of the occurrence around the circumstance. 8 current directions for each 2D current profiles are applied, refer to Figure 21.

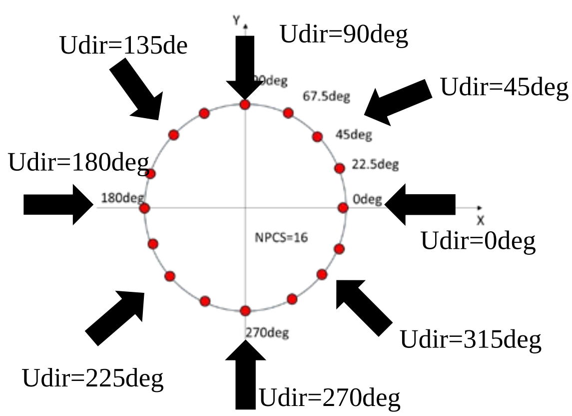

Figure 21 Current directions

The fatigue life along the riser can be calculated following the equation below:

$$\boldsymbol{life(z,ip) = 1/\left(\frac{1}{8}\sum_{ic=1}^{21}\left(\sum_{ih=1}^{8} Dam(z,ip,ic,ih) * p(ic)\right)\right)}$$

where $Dam(z, ip, ic, ih)$ represents fatigue damage at riser location , point ip around the circumstance for current profile ic and heading ih.

The fatigue life estimated from two methods are presented in Figure 22.

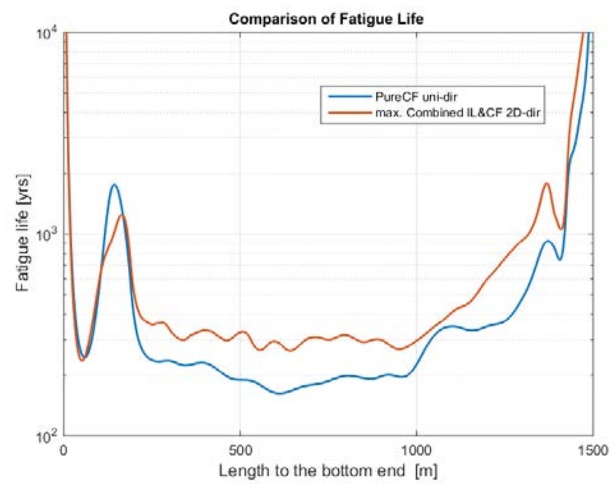

Figure 22 Comparison of predicted minimum fatigue life of a TTR based on pure CF response analysis with uni-directional current profiles and combined IL&CF response analysis with 2D directional current profiles

The minimum fatigue life based on pure CF response analysis is about 70% of the result based on combined IL&CF response analysis using 2D directional current. The difference is larger at the middle of the riser with a factor of 2. It is also noted that the combined IL&CF response using 2D directional current can give lower fatigue life locally, i.e. 50 m from the bottom end.

CONCLUSIONS

In the present study, the existing combined IL and CF response load model in empirical VIV prediction program VIVANA has been validated against the NDP VIV model test results. The present model gives accurate prediction of CF and IL responses and fatigue damage. A reliable combined CF and IL response calculation enables VIV prediction subjected to 2D directional current profiles.

A case study of a deep water top tensioned riser has been carried out to examine the differences in VIV fatigue damage calculation using uni-directional and 2D directional current profiles. The 8 current headings are assumed to have equal probability of occurrence around the circumstance of the riser cross-section. It is shown that fatigue life of the riser is under-predicted by pure CF analysis using uni-directional current profiles by 30%. The difference may be more significant if the current heading has un-even probability of occurrence. The combined IL and CF response analysis gives less conservative estimation of the fatigue life with more realistic 2D directional current profiles.

ACKNOWLEDGMENTS

The authors are grateful to the Norwegian Deepwater Program (NDP) for its permission to use the experimental data in this study.

REFERENCES

[1] Baarholm, G., Larsen, C.M., Lie H., On fatigue damage accumulation from in-line and cross-flow vortex-induced vibrations on risers Journal of Fluids and Structures 22 (2006) 109–127.

[2] Baarholm, G.S., Larsen, C.M. and Lie, H.: "Effect of strakes on fatigue damage due to cross-flow VIV" 3rd International conference on hydroelastisity in marine technology, Wuxi 2006

[3] Chaplin, J. R., Bearman, P. W., Huera Huarte, F. J. and Pattenden, R. J., 2005. Laboratory measurements of vortex-induced vibrations of a vertical tension riser in a stepped current. Journal of Fluids and Structures, 21, 3-24.

[4] Dahl, J. M. (2008), Vortex-Induced Vibration of a Circular Cylinder with Combined In-line and Cross-ow Motion, Doctor of philosophy, Center for Ocean Engineering, Department of Mechanical Engineering, MIT, Webb Institudte, Glen Cove, NY, USA.

[5] Gopalkrishnan, R. (1992). Vortex-Induced Forces on Oscillating Bluff Cylinders. Cambridge, MA, USA: Massachusetts Institute of Technology.

[6] Huse, E., Kleiven, G. and Nielsen, F. G., 1998. Large scale model testing of deep sea risers. In: Proceedings of the Offshore Technology Conference, OTC-8701, Houston, USA.

[7] Passano, E., Lie, H., Larsen, C.M., Comparison of calculated In-line vortex induced vibrations to model tests. Rio de Janeiro, Brazil, 31st International Conference on Ocean, Offshore and Arctic Engineering, OMAE2012-83387.

[8] Passano, E., Larsen, C.M., Lie, H., and Wu, J., (2014a) VIVANA - Theory Manual Version 4.4.

[9] Passano, E., Larsen, C.M. and Wu, J. (2014b), On prediction of fatigue damage from VIV. San Francisco, California, USA, 33rd International Conference on Ocean, Offshore and Arctic Engineering, OMAE2014-24217.

[10] Soni, P. K., 2008. Hydrodynamic coefficients for vortex induced vibrations of flexible beams. D. Sc. Thesis, Department of Marine Technology, NTNU, Trondheim, Norway.

[11] Srivilairit, T. and Manuel, L., Vortex-Induced Vibration and Coincident Current Velocity Profiles for a Deepwater Drilling Riser. *J. Offshore Mech. Arct. Eng* 131(2), 021101 (Feb 26, 2009)

[12] Trim, A. D., Braaten, H., Lie, H. and Tognarelli, M. A., 2005. Experimental investigation of vortex-induced vibrations of long marine risers. Journal of Fluids and Structures, 21, 335-361.

[13] Triantafyllou, M., Triantafyllou, G., David Tein, Y. S., & Ambrose, B. D. (1999). Pragmatic riser VIV analysis. Houston, USA: Offshore Technology Conference.

[14] Vandiver, J., & Li, L. (2007). Shear7 v4.5 Program Theoretical Manual. Cambridge: Massachusetts Institute of Technology.

[15] Vikestad, K., Larsen, C., & Vandiver, J. (2000). Norwegian Deepwater Program Damping of Vortex-Induced Vibrations. Offshore Technology Conference, OTC11998. Houston, USA.

[16] Voie, P., Wu, J., Larsen, C.M., Resvanis,T., Vandiver, K., and Triantafyllou, M., Consolidated guideline on analysis of vortex-induced vibrations in risers and umbilicals, Trondheim, 36th International Conference on Ocean, Offshore and Arctic Engineering, OMAE2017-61362.

[17] WAFO-group (2000). "WAFO - A Matlab Toolbox for Analysis of Random Waves and Loads - A Tutorial" Math. Stat., Center for Math. Sci., Lund Univ., Lund, Sweden.

[18] Wu, J., 2011, Hydrodynamic Force Identification from Stochastic Vortex Induced Vibration Experiments with Slender Beams, PhD Dissertation, Norwegian University of Science and Technology, Trondheim.

[19] Wu, J., Lie, H., Larsen, C. M., Liapis, S. and Baarholm, R., Vortex-induced vibration of a flexible cylinder: Interaction of the in-line and cross-flow responses. Journal of Fluids and Structures 63:238-258, May 2016.

[20] Wu, J., Larsen, C. M. and Lie, H. (2010), Estimation of hydrodynamic coefficients for VIV of slender beam at high mode orders, 29th International Conference on Ocean, Offshore and Arctic Engineering', Shanghai, China.

[21] Yin, D., 2013, Experimental and Numerical Analysis of Combined In-line and Cross-flow Vortex Induced Vibrations, PhD Dissertation, Norwegian University of Science and Technology, Trondheim.

ANNEX A RISER DATA

Water depth	1500	m
Upper end	12	m
Lower end	-1500	m
Total length	1512	m
Density, pipe	7.85	t/m^3
Mod of elasticity	206000	MPa
Density int. fluid	1.4	t/m^3
Density sea water	1.025	t/m^3
Tension at low. end	400	kN

Bare riser data

External diameter	0.6	m
Wall thickness	0.02	m
Internal diameter	0.56	m
Needed top tension	5493.3	kN
EI	316051	kN/m^2
EA	7507150	kN/m

Buoyancy zone data

Upper end bel. Surface	75	m
Lower end above bottom	190	m
Total length buoyancy section	1235	m
External diameter	1.0	m
Density of material	0.4	kg/m^3
Mass of buoyancy material	0.2011	t/m

Boundary conditions

	Top end	Bottom end
displ, x	fixed	fixed
displ, y	fixed	fixed
displ, z	free	fixed
rot, x	free	free
rot, y	free	free
rot, z	fixed	fixed